

## Research Article

# Comparative Evaluation of the Adsorption Performance of Citric Acid-Treated Peels of *Trapa natans* and *Citrullus lanatus* for Cationic Dyes Degradation from Water

Muhammad Sadiq Hussain, Rabia Rehman , and Muhammad Imran

Centre for Inorganic Chemistry, School of Chemistry, University of the Punjab, Quaid-e-Azam Campus, Lahore-54590, Pakistan

Correspondence should be addressed to Rabia Rehman; [grinorganic@yahoo.com](mailto:grinorganic@yahoo.com)

Received 3 January 2022; Revised 2 March 2022; Accepted 16 April 2022; Published 20 May 2022

Academic Editor: Beatriz P. P. Oliveira

Copyright © 2022 Muhammad Sadiq Hussain et al. This is an open access article distributed under the Creative Commons Attribution License, which permits unrestricted use, distribution, and reproduction in any medium, provided the original work is properly cited.

Various chemicals were explored in chemical combinations with two selected agrowastes in order to optimize, enhance, and improve their biosorption potential for the optimal and effective eradication of noxious, carcinogenic, and malignant cationic and basic dyes from wastewater. In this project, environmentally safe, economic, inexpensive, and widely available peels of *Trapa natans* (TP) and *Citrullus lanatus* (CP) were collected, dried, and pretreated with citric acid, revealing promising results. FT-IR and SEM characterizations of chemically changed biosorbents (C-TP and C-CP) have evidenced the presence of more secondary adsorption sites on their surfaces. These acid-modified biosorbents were employed to eliminate the hazardous and toxic basic dyes such as Rhodamine B (RAD) and Brilliant Green Dye (BLG) in batch mode processing. The Langmuir model was best fitted to equilibrium experimental data as compared to Freundlich and Temkin isothermal mathematical models with  $Q_{\max}$  of 15.63 and 27.55 mg/g for RAD using C-TP and C-CP, respectively, whereas, for BLG on C-TP and C-CP, it was 128 and 189 mg/g, respectively. Therefore, the mechanism is related to chelation and ion exchange modes between adsorbate molecules and adsorbent surfaces, leading to homogeneous and monolayer adsorption and following pseudo-2nd-order kinetics in the best way. Thermodynamic parameters such as  $\Delta G^0$ ,  $\Delta S^0$ ,  $\Delta H^0$ , and  $\Delta E^0$  are determined statistically for the adsorption performance of both novel chemically mutant biosorbents, which reflect that biosorption mechanisms are exothermic as well as spontaneous.

## 1. Introduction

The most severe and alarming ecological worldwide threat is water pollution, which deteriorates the water quality. Textile, fabrics, and printing industrial processing units discharged about 10–15% coloring matters into water bodies, which persist for an extended time span due to nonbiodegradable ability [1]. Dyes consumption in textile industrial units is more than 10000 tons per annum on global level, whereas, according to an estimate after dyeing process, their wastewater comprises dyes effluents about 1000 tons per annum which has a significant role in contaminating water resources [2, 3]. Unprocessed or partially treated dyestuffs containing industrial water have serious adverse effects on natural ecosystem and severely damage the water resources ultimately and cause the complicated health problems in

mankind and increase in mortality rate per annum [4]. The dyes mostly persist in water for extended period of time and even in traces are easily visible and can be identified in water [5]. Organic dyes such as azo dyes on introduction in human body can cause tumors and bladder cancer, due to destruction of DNA molecules [6]. Previous investigations revealed that drinking water containing dyes effluents like Rhodamine B (RAD) and Brilliant Green Dye (BLG) has highly toxic, carcinogenic, hazardous, and severe mutagenic effects on human bodies [7] and leads to acute poisoning, gastrointestinal problems, liver dysfunction, breath shortness, infections in respiratory tract, and skin dermatitis [7]. Therefore, it is the requirement of time to get rid of such toxic, hazardous, lethal, mortal, and incurable effluents from water streams to save the precious lives of infants and people. Different techniques including physical and chemical

methods such as electrochemical oxidation, precipitation, ozonolysis, coagulation-flocculation, and ion exchange have been employed to eradicate the dyestuffs from water but most of them are complicated and highly sensitive to environmental factors, prolong operational time, are costly, and generate hazardous byproducts [8, 9]. In this investigation, biosorption, the most emerging technique, is employed to remove hazardous and toxic dyes from water. This technique is widely explored because raw materials (agrowaste) are usually eco-friendly, cheap, easy to use, and easily available for removing any type of contaminants from water. In previous investigations, agrowastes like *Dalbergia sissoo*-activated carbon [10], raw pomegranate peels [11], raw timber wood sawdust [12], nitric acid-treated pine cone [13], banana peels [14], and jackfruit peels [15] had given efficient adsorptive removal outcomes for RAD, while for the adsorptive eradication of BLG areca nut husk [16], *Sesamum indicum* tree waste [17], almond shells [16], date pits-activated carbon [3], tree wood of guava-activated carbon [18], and rice husk [19] were utilized as biosorbents. It was observed from reported data that chemically processed biosorbents had shown good and promising results as compared to the raw and untreated forms. In the consideration of previously reported results of biosorption of dyes, two cheap, eco-friendly, abundant, and easily accessible agrowastes, TP and CP, have been selected for the expulsion of toxic and hazardous RAD and BLG from wastewater. The main objective of this investigation is to alter the surface morphology of the lignocellulosic biomass by providing additional active adsorption binding sites for the associations with the dye molecules from wastewater. After treatment with the most suitable modifying agent, the adsorbents will become more efficient and quicker to eradicate the dyestuffs from the water. In this study, the selected biosorbents will be chemically modified by using different chemicals (solvents and chelating agents) to assess their adsorption performance and efficiency for the removal of selected dyes under suitable operating conditions.

## 2. Materials and Method

**2.1. Chemicals and Glass Apparatus.** In this study, pure chemicals and reagents were acquired from well-known and high reputed companies Merck and Fluka, which were BLG- $\lambda_{\max}$  of 625 nm, RAD- $\lambda_{\max}$  of 554 nm, urea, thiourea, EDTA, hydrochloric acid, sulfuric acid, nitric acid, sodium hydroxide, sodium carbonate, sodium chloride, potassium iodide, iodine, indicators, (R-OH) methyl, ethyl, and Isopropyl alcohols, propanone, organic acids chelating agents like lactic acid, citric acid, and tartaric acid, while glassware were made of Pyrex, were washed with deionized distilled water, and were sterilized for 30 min. at 80°C in electrical oven.

**2.2. Methodology for the Preparation of Raw Biosorbents.** The biosorbents selected for this investigation are eco-friendly, nontoxic, and easily accessible locally. The peels of both biosorbents, *Trapa natans* (TP) and *Citrullus lanatus*

(CP), were acquired from Lahore and nearby areas and, thereafter, washed with running water to remove entrapped dust and other waste matters. The peels of both adsorbents were trimmed with a sharp knife into suitable sizes for experiments and then carefully washed with distilled water. Later, the peels were dried in sunlight for ten days and placed in an oven at about 70°C for 72 hours to remove the entrapped moisture in the first phase. After literature survey, the peels were ground and sieved to a 70-mesh size, resulting in fine powder [20]. These powdered peels were again dried in an oven for 24 hours to remove further entrapped moisture in the second phase and were placed in plastic jars labelled as TP and CP for use in adsorption experimental investigations. Flow sheet diagram for the preparation of raw biosorbents is elaborated in Figure 1.

**2.3. Characterization of Biosorbents.** TP and CP were analyzed through different techniques like Boehm titration for identification of acidic/basic moieties, pH, % age of moisture and ash contents, elemental and volatile matters determinations, estimation of porosity/bulk density, and iodine titration as listed in Table 1 [21].

**2.4. Chemical Treatment of Biosorbents.** The surface morphologies of both biosorbents (TP and CP) were chemically amended by using different modifying agents such as different kinds of alcohols (methyl, ethyl, and isopropyl alcohols), acetone, mineral acid like HCl, caustic soda (NaOH), numerous chelating agents like EDTA, urea, thiourea, and organic acids (citric acid, lactic acid, and tartaric acid). The chemistry of treatment of biosorbents with different chemicals was categorized in two phases.

Phase I: chemical processing with different solvents:

100 g of each biosorbent was placed in 250 mL of each solvent in Erlenmeyer flasks sealed with Al-foil for 6–10 hours at 30°C on an orbital shaker at 150 rpm. Extra and excessive soaking in solvent-based modifying agents was avoided to protect the raw adsorbents from deterioration and decay, especially in the cases of alkali and acids. The content in each flask was filtered and washed with distilled and deionized water carefully to remove entrapped solvent molecules. Afterward, the chemically modified biosorbents were dried for 24 hours at 80°C in an electric oven and then stored in plastic jars for further experimental work.

Phase II: chemical processing with different chelating agents:

To increase the additional active adsorption binding sites on the interfaces of both raw biosorbents (TP and CP), solid phase chemical modification was carried out by using different chelating agents. For this purpose, 54 g of each powdered biosorbent, TP and CP, was thoroughly mixed with 6 g of each chelating agent in different China dishes separately. Each China dish was wrapped in aluminum foil and microwave-irradiated for 8–10 minutes [22]. The chemically treated

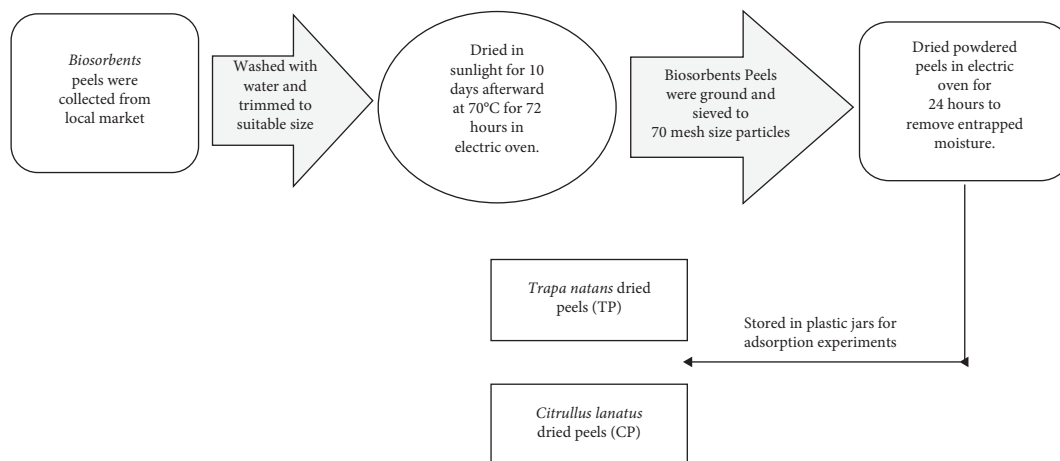


FIGURE 1: Schematic diagrams for the preparation of raw adsorbents.

TABLE 1: Physicochemical characterization of both biosorbents.

Evaluation of parameters	TP values	CP values
pH	5.6	5.9
Particle density ( $\text{g}\cdot\text{cm}^{-3}$ )	0.588	0.479
Bulk density ( $\text{g}\cdot\text{cm}^{-3}$ )	0.5	0.96
Percentage of ash content	6.8	2.4
Percentage of moisture content	7.7	8.3
Percentage of porosity	0.78	0.2
Percentage of volatile organic components	89.7	5.6
Iodine number ( $\text{mg}\cdot\text{g}^{-1}$ )	15.5	2.1
Phenolic moieties (millimoles)	0.0841	0.0038
Lactones (millimoles)	0.0592	0.0056
Carboxylic acids (millimoles)	0.0391	2.442
Surface basic sites (millimoles)	0.0048	2.011

adsorbents were carefully stored in plastic jars for further experimentation. These chemically modified adsorbents were tested under optimized operational conditions for the adsorption removal of RAD and BLG from water bodies in a batch mode investigation.

**2.5. Experimental Investigations on Biosorption.** The maximum adsorptive removal of both basic dyes (RAD and BLG) was promising with the citric acid-treated novel adsorbents during the batch mode experiments. The native TP after chemical treatment and amendment was labeled as C-TP, whereas native CP was labeled as C-CP for further studies. During the experimental approach, for each experiment, 25 ppm of each of the RAD and BLG solutions was prepared and 25 mL of each solution was taken in 100 mL conical flasks to optimize the operational factors for adsorption studies. The chemical structures of two basic (cationic) model dyes selected for their elimination from wastewater are shown in Figures 2 [23] and 3 [24], respectively.

**2.5.1. Optimization of Operational Parameters.** During the biosorption experimental comparative studies, various operational parameters, such as biosorbent dosage range

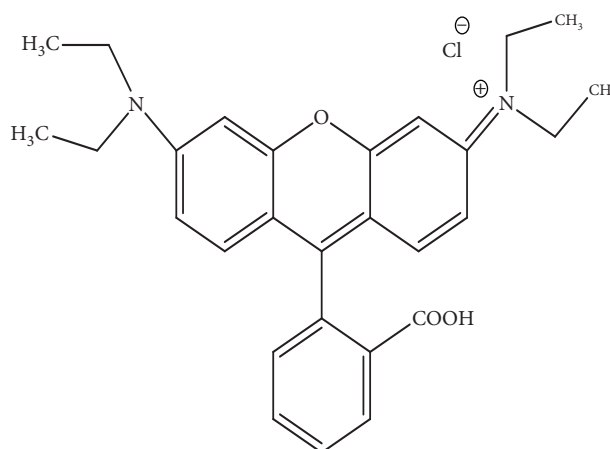


FIGURE 2: Chemical structure of Rhodamine B.

(0.2–2.0 g with difference 0.1 g), pH range (1–10), temperature range (10–80°C), and contact time range (5–60 minutes), as well as shaking speed range (25–200 rpm with gap of 25 rpm), were optimized to get better results. Mathematical modeling for isothermal and kinetic equilibria investigations was also determined to analyze and manipulate the reliability of the adsorption results. The % age adsorption of both dyes by using modified adsorbents was determined from the relation given in the following equation [25]:

$$\% \text{Adsorption} = \left( \frac{C_o - C_e}{C_o} \right) \times 100. \quad (1)$$

The amounts (mg/g) of adsorbed dyes were determined from the following equation [26]:

$$Q = \left[ \frac{(C_o - C_e)V}{W} \right]. \quad (2)$$

In the above relations, for each adsorbent,  $Q$  is amount of dyes (mg/g),  $C_o$  represents initial concentration (ppm),  $C_e$  is concentration (ppm) in equilibrium of both RAD and BLG,  $V$  is volume in  $L$ , and  $W$  is mass in grams.

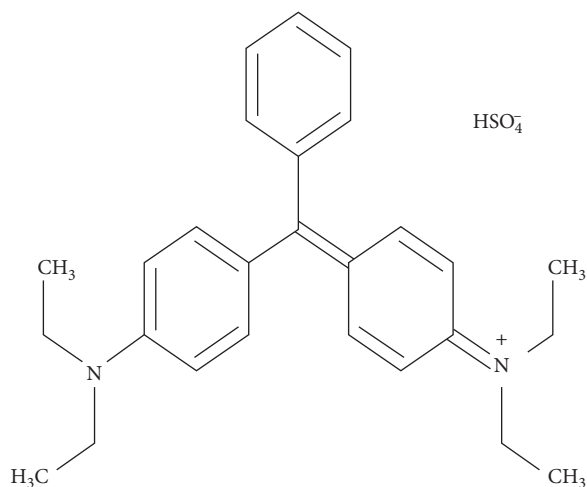


FIGURE 3: Chemical structure of Brilliant Green Dye.

### 3. Results and Discussion

The biosorbents were chemically modified with numerous modifying agents as mentioned in Section 2.4. After the performance of many repeatedly experiments, the most suitable modifying agent was selected for the amendment of surface morphology of TP and CP. The characterization of adsorbents was carried out through FT-IR and SEM. The validity and reliability of equilibrium data were evaluated by Langmuir, Freundlich, Temkin, and kinetics modeling.

**3.1. Chemical Modification of Biosorbents.** The raw biosorbents TP and CP were chemically treated with different chemicals, including various organic solvents, acids, alkalis, and chelating agents, as mentioned in experimental Section 2.4. The adsorption performance of chemically processed biosorbents with different chemicals was assessed for the removal of RAD and BLG from the water system. It was observed after repeated experiments that citric acid-treated TP and CP performed better and showed maximum adsorptive removal of RAD and BLG, as elaborated in Figure 4. It was evidenced from FT-IR and SEM analysis that citric acid has been esterified with the OH groups on the surfaces of biosorbents and has provided extra and additional adsorption sites to associate with dye molecules from aqueous solutions. Therefore, enhanced active binding sites on modified biosorbents surfaces have contributed to efficient and quick adsorption equilibria at the interface of adsorbate-adsorbents.

The maximum adsorptions of RAD on citric acid-modified adsorbents C-TP and C-CP at optimum conditions were found to be 91% and 96%, respectively, whereas for BLG on C-TP and C-CP they were 88% and 92%, respectively, which were promising as compared to other utilized chemicals. Solid phase chemical modification treatment of raw biosorbents (TP and CP) with citric acid under microwave irradiation was performed as mentioned in Section 2.4.

### 3.2. Spectroscopic Analysis

**3.2.1. FT-IR Analysis of Chemically Processed Adsorbents.** 0.8 g of each C-TP and C-CP had been placed separately in four conical flasks containing 25 mL solutions of RAD and BLG with 25 ppm conc. for 20 minutes at 125 rpm and 30°C. After adsorption, each sample was filtered and the residue was dried for FT-IR evaluation. Figure 5 represents a comparative study of *Trapa natans* peels, native form (TP), and after chemical treatment with citric acid (C-TP). The region between 3900 and 3600  $\text{cm}^{-1}$  indicated the surface modification under the influence of esterification between free OH moieties of alcohols on TP and modifying agent citric acid. A broad band at 3300  $\text{cm}^{-1}$  showed the COOH moieties on TP which was obviously changed after treatment and, similarly, a high amendment between 1395 and 1440  $\text{cm}^{-1}$  in C-TP as compared to TP is a good signal for additional COOH groups which had played promising role during adsorption.

The region between 1330 and 1415  $\text{cm}^{-1}$  reflected the OH bending for alcohols. Thus, the modified spectra of TP had more and additional carboxylic acid groups for the efficient and quicker adsorption of selected dyes. Figure 6 expresses a comparative study of *Citrullus lanatus* peels, native form (CP), and after chemical processing with citric acid (C-CP). The region between 3850 and 3650  $\text{cm}^{-1}$  on C-TP showed the surface chemical alteration due to reaction between free OH groups on TP and modifying agent citric acid.

A reduced broad band at 3500–3200  $\text{cm}^{-1}$  on C-TP as compared to CP showed intermolecular bonded forces of citric acid with free OH moieties. A changed frequency at the region between 3000 and 2700  $\text{cm}^{-1}$  on C-CP represented the COOH moieties, while wavenumber (1778–1745) indicated the COOH and esterified groups of citric acid molecules in C-TP. The new peaks in the range of 1435–1400  $\text{cm}^{-1}$  in C-TP as compared to TP associated with OH bending groups of carboxylic acids, which had played good role during adsorption of dyes. The region of 1260–1100  $\text{cm}^{-1}$  reflected ester linkage. Therefore, the amended morphology of TP after chemical treatment shown in C-TP in Figure 6 had provided numerous (COOH) groups for the better and quicker adsorption equilibria in aqueous solutions of RAD and BLG.

**3.2.2. FT-IR Analysis after Adsorption of Dyes.** Figure 7 depicts the FT-IR spectra of model dyes RAD and BLG following adsorption on citric acid-treated adsorbents C-TP and C-CP.

Figures 7(a) and 7(b) show the FT-IR spectra following the adsorption of the first model dye, RAD, on C-TP and C-CP, respectively. The change in wavenumber in the case of C-TP after adsorption of RAD at 3875, 3730, and 3610  $\text{cm}^{-1}$  in Figure 7(a) and for C-CP at frequencies of 3902, 3855.5, and 3737  $\text{cm}^{-1}$  in Figure 7(b) reflects the adsorption under the influence of strong intermolecular hydrogen bonding caused by the involvement of the O-H group of -COOH moieties with the dye molecules, while peaks between 3390 and 3200  $\text{cm}^{-1}$  in Figure 7(a) and between 3330 and

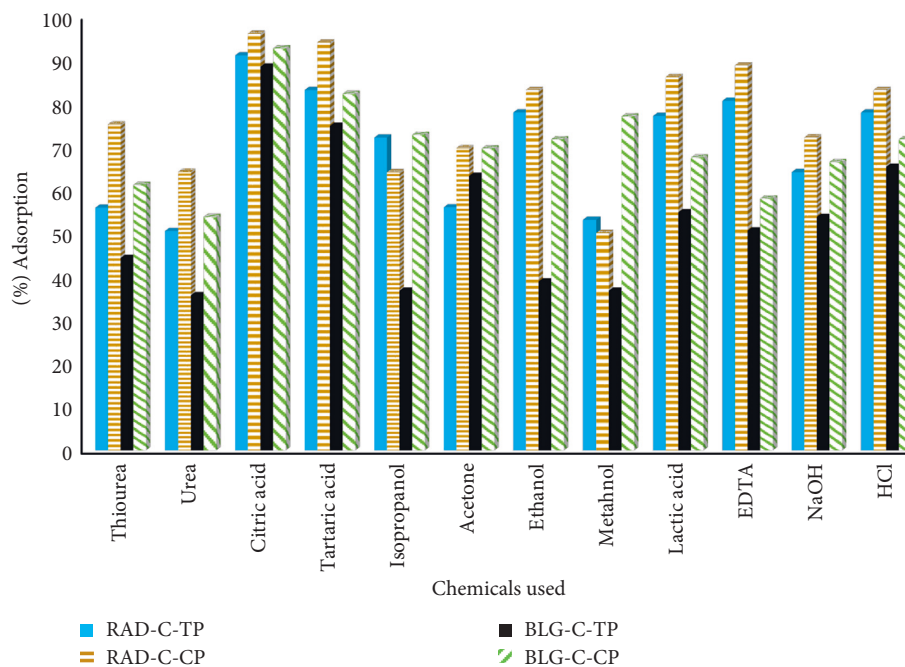


FIGURE 4: A comparative study of adsorption of dyestuffs after chemical modification with different modifying agents.

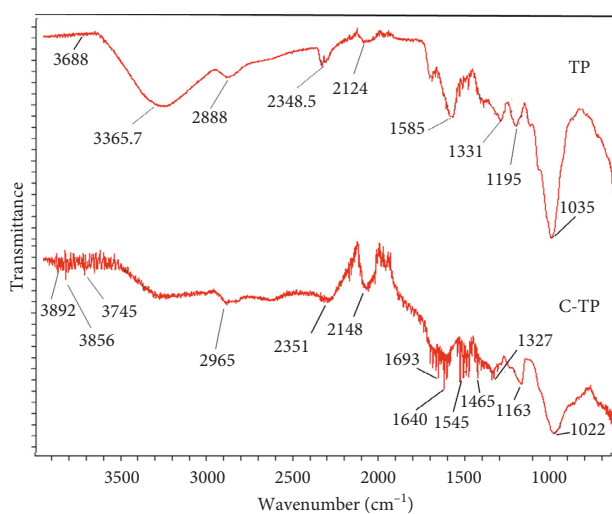


FIGURE 5: A comparative FT-IR analysis of native (TP) and citric acid-modified (C-TP) *Trapa natans* peels.

3250  $\text{cm}^{-1}$  in Figure 7(b) indicate interactions with RAD caused by the -OH group of carboxylic acid on acid-modified adsorbents C-TP and C-CP, respectively. Figures 7(c) and 7(d) show the FT-IR spectra following the adsorption of the second model dye, BLG, on C-TP and C-CP, respectively. In both cases, the change in wavenumber at 3900, 3845, and 3740  $\text{cm}^{-1}$  in Figure 7(c) and at 3900, 3820, and 3700  $\text{cm}^{-1}$  in Figure 7(d) indicate significant intermolecular interactions between BLG and the citric acid-modified adsorbents C-TP and C-CP. The wavenumber at 1800–1570  $\text{cm}^{-1}$  in 7(c) and 1760–1520  $\text{cm}^{-1}$  in 7(d) associated with the adsorption of BLG. It was noticed from previously reported data that functional groups containing oxygen promote the adsorption of cationic dyes [27–29]. The

prominent peaks in Figure 7(c) at 1437  $\text{cm}^{-1}$  and in Figure 7(d) at 1440  $\text{cm}^{-1}$  illustrate (OH) bending groups for COOH moieties on modified adsorbents C-TP and C-CP, respectively.

**3.2.3. SEM Analysis of Modified Adsorbents.** The unprocessed TP in Figure 8(a) has packed tubular shapes gaps and voids, while its chemically amended form using citric acid C-TP in Figure 8(b) has irregular tubular, granular, and honeycomb-like arrangements with increased surface area. This revealed that the morphology of native TP had been modified which favored and provided enhanced additional binding linkages, surface area, and adsorption sites for adsorptive elimination of selected dyes from water. The structural morphology of raw CP is depicted in Figure 8(c), with gaps, tiny imprinted depressions in between the many spherical bodies, and dense circular clusters. Figure 8(d) shows a chemically modified citric acid-treated form of CP. It is converted into fleece lined, flossy, granular, frizzy, and frothy bodies with numerous binding sites for efficient, quicker, and good adsorptive removal of RAD and BLG from aqueous solution. Figure 8(d) shows an aggregate of clusters of citric acid molecules on the interface of C-CP. The modified surface morphology of both C-TP and C-CP with numerous available active adsorption sites promotes adsorption phenomenon as compared to their unprocessed forms which is reported in different investigations and shown in Table 2.

**3.3. Optimization of Operational Conditions.** Parameters settings for experiments like  $T$  ( $^{\circ}\text{C}$ ), biosorbent dosage, retention time, stirring rate, and pH of solution were used to determine the best conditions for adsorptive eradication of



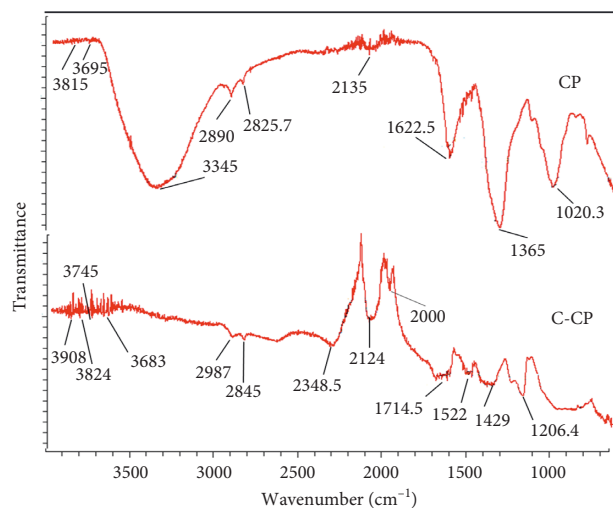


FIGURE 6: A comparative FT-IR analysis of native (CP) and citric acid-modified (C-CP) *Citrullus lanatus* peels.

RAD and BLG by using citric acid-modified adsorbents C-TP and C-CP, respectively.

**3.3.1. Modified Adsorbent Dosage Effect on Adsorption.** The adsorbent dose of C-TP and C-CP ranged from 0.2 to 2.0 g, with a difference of 0.1 g being utilized under different operational conditions.

According to FT-IR interpretation, citric acid-modified adsorbents C-TP and C-CP with additional COOH groups have more active binding affinity on their interfaces for association with cationic dye molecules RAD<sup>+</sup> and BLG<sup>+</sup>. For this study, 25 ppm solutions with a volume of 25 mL were taken separately in four sets of Erlenmeyer flasks, and each set contained ten flasks for smooth experimental studies. The experimental operational conditions for the study of adsorption dose investigation were employed as follows: temperature of 30°C, 125 rpm agitation speed, initial pH = 5, and final pH for RAD on C-TP and C-CP = 4, whereas for BLG on C-TP it was 4.5 and for BLG on C-CP it was 4. Figure 9 depicts the experimental results graphically. For 0.8 g of C-TP, the maximum RAD adsorptive removal from aqueous solution was 91.5 percent, and, for 0.8 g of C-CP, it was 96.8 percent. Similarly, the maximum adsorptive elimination of the second model dye, BLG, was determined to be 96.84 percent on 0.8 g of C-TP and 98.94 percent on 0.8 g of C-CP. Figure 9 also illustrates that, at low concentrations, the adsorption of each model dye, RAD and BLG, increases due to a greater number of available binding adsorption sites on the acid-treated biosorbents, but as concentration increases, the equilibrium between adsorbates and adsorbents interfaces is quickly established, resulting in decreased adsorption [45]. The optimal adsorbent dose of 0.8 g was determined for further experimental studies.

**3.3.2. Contact Time Influence on Adsorption.** As shown in Figure 10, the performance of the adsorption process is related to the contact time interval and the number of available binding sites on the interfaces of biosorbents C-TP

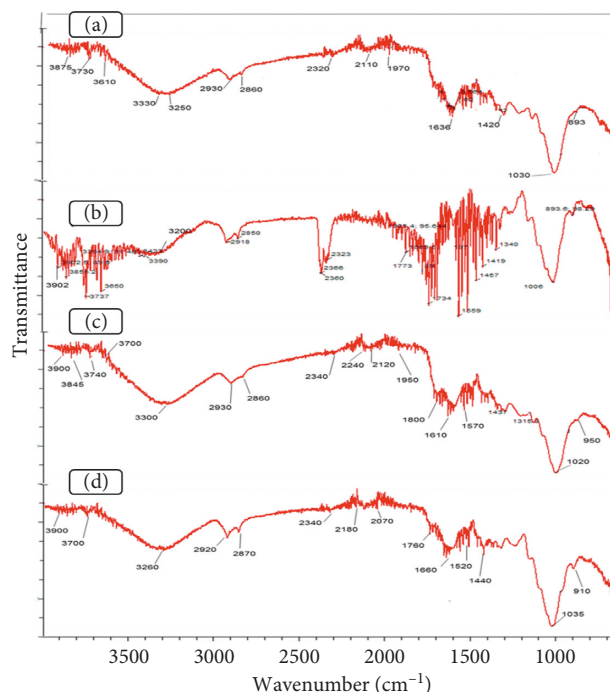


FIGURE 7: FT-IR spectra after adsorption of RAD and BLG. (a) RAD-C-TP. (b) RAD-C-CP. (c) BLG-C-TP. (d) BLG-C-CP.

and C-CP. Initially, with the increase in contact time interval, the adsorption of RAD and BLG enhanced till the optimal time interval was achieved and afterward decreased by unit mass due to the establishment of equilibrium and many vacant adsorption binding sites left on the surfaces of C-TP and C-CP. A contact time duration of 60 minutes with a difference of 5 minutes was selected for this study by using 25 mL of each of RAD and BLG solutions with a concentration of 25 ppm. The optimal time interval for maximum adsorption removal of RAD on C-TP was 91.51% at 25 minutes, while for BLG on C-TP it was 93.68% at 25 minutes, whereas the adsorptive eradication from aqueous solution of RAD on C-CP was 96.99% at 20 minutes, while for BLG on C-CP it was 97.89% at 20 minutes as illustrated in Figure 10. By comparing the results of citric acid-modified biosorbents with the previously reported data as tabulated in Table 2, the efficiency of the adsorption performance of C-TP and C-CP is promising due to the accessibility of RAD and BLG toward extra adsorption active sites and intra-particle diffusion [46]. Moreover, after the optimal time interval and with the passing of time period, the overabundance of the RAD and BLG cations on the surfaces of C-TP and C-CP induces reduction and a cessation of the efficiency of the adsorption performance [28]. Therefore, the optimal contact time interval of 20 minutes was determined for further experimental work.

**3.3.3. Influence of Agitation on Adsorption.** It is another significant factor that controls the adsorption behavior because it results in the formation of a light coating of adsorbates (RAD and BLG) on adsorbents from solutions. The formation of a distinctive and different outermost

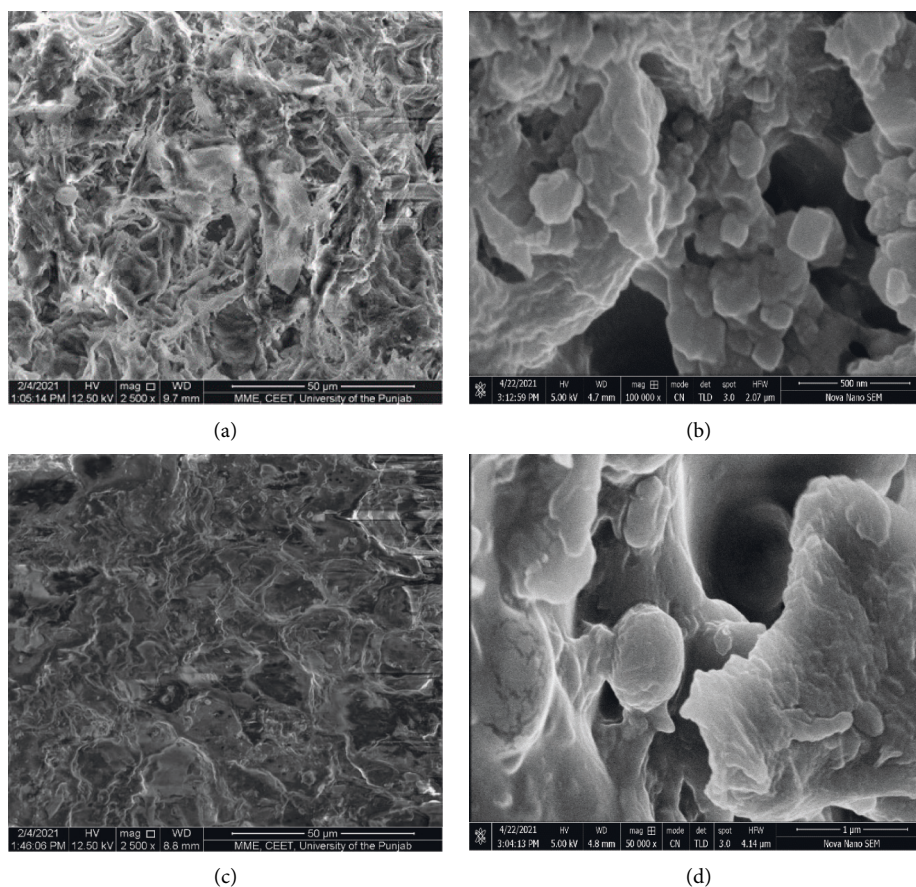


FIGURE 8: A comparative SEM evaluation. (a) TP, (b) C-TP, (c) CP, and (d) C-CP.

boundary of cationic dye molecules on modified adsorbents boosts and promotes adsorption performance [47]. Therefore, agitation rate influenced the adhering of RAD and BLG on citric acid-modified C-TP and C-CP. This factor was studied in the range of 25 to 200 rpm speed with just difference of 25 rpm. Experiments in batch mode were carried out under other appropriate operating parameters such as contact time of 20 minutes, temperature of 30°C, 0.8 g adsorbent dose, initial pH of 5, and the conc. of each dye solution of 25 ppm with a 25 mL volume.

As a consequence, maximal decontamination of RAD on C-TP and C-CP was 91 and 92.6% at 125 rpm agitation speed, whereas maximum adsorptive reduction of BLG on C-TP was 97% at 125 RPM and that on C-CP was 96% at 100 RPM, as graphically shown in Figure 11. During the experiment, high RPM speed was observed to be connected to a decrease in the adsorption process owing to the creation of excessive uniform circular motion velocity of independent RAD and BLG molecules from water [48], which can also be seen in Figure 11.

**3.3.4. Influence of Temperature Variations on Adsorption.** The adsorption mechanism can be exothermic or endothermic, and it is strongly linked to temperature fluctuations, which can be seen in Figure 12.

Temperature changes influence the kinetic energy of dye molecules, which ultimately change the thermodynamic parameters. According to the literature, adsorption is generally temperature-dependent, so higher temperatures decrease the rate of the adsorption process [48]. The impact of temperature varying from 10 to 80°C with just a 10°C gap was examined for optimization of the aforementioned parameters during this study by using a 25 mL volume of each RAD and BLG separately, with a concentration of 25 ppm under optimized conditions. The highest adsorption percentage expulsion of RAD on C-TP was 89% at 40°C and on C-CP it was 94% at 30°C, while the maximal percentage removal of BLG on C-TP and C-CP was 90.5% and 97%, respectively, at 30°C. The adsorption of dyes rises at certain high temperature levels, as mentioned in Figure 12, because the adsorbent framework is degraded and disrupted by the high temperature. As a consequence, in such cases, the adsorbents expand, bulge, and elongate. Consequently, dyes (RAD and BLG) penetrate deeper into the deteriorated structure of the adsorbents [49]. Hence, the rate of adsorption accelerates. As a consequence, in some cases, adsorption increases at high temperature variations, such as RAD adsorption on C-TP rising from 50 to 60°C (78 to 83%), RAD adsorption on C-CP continuing to increase from 60 to 70°C (67 to 72%), and BLG adsorption on C-TP increasing

TABLE 2: A comparison of the adsorption capacity with some previously published works.

Biosorbents	Adsorption capacity (mg/g)	References
<i>Detoxification of Rhodamine B dye</i>		
<i>Rhizophora mucronata</i> , carbon nanotubes composite	6.784	[30]
<i>Gracilaria edulis</i>	8.96	[31]
<i>Kappaphycus alvarezii</i>	9.84	[31]
<i>Gracilaria salicornia</i>	11.03	[31]
Crude coconut fibers	13	[32]
HCOOH-modified coconut fibers	22	[32]
<i>Artocarpus heterophyllus</i> seed	26.4	[33]
Hexadecyltrimethylammonium bromide-treated <i>Volvariella volvacea</i>	33.51	[34]
Acrylic acid-processed walnut shell	48.87	[35]
Inactivated <i>Aspergillus oryzae</i>	98.59	[36]
<i>Elaeis guineensis</i> shell	108	[37]
<i>Trapa natans</i> peels modified with citric acid	15.63	Current research work
<i>Citrullus lanatus</i> peels modified with citric acid	27.55	Current research work
<i>Detoxification of Brilliant Green Dye</i>		
Peanut shells	19.92	[38]
Raw peels of <i>Trapa natans</i>	50.51	[39]
Rock melon skin	118	[40]
Snail shell-rice husk	129.8	[41]
White rice husk ash	85.56	[42]
Cellulose (raw)	90.5	[43]
H <sub>3</sub> PO <sub>4</sub> -treated cellulose	150	[43]
Banana peels	22.44	[44]
<i>Trapa natans</i> peels modified with citric acid	128	Current research work
<i>Citrullus lanatus</i> peels modified with citric acid	189	Current research work

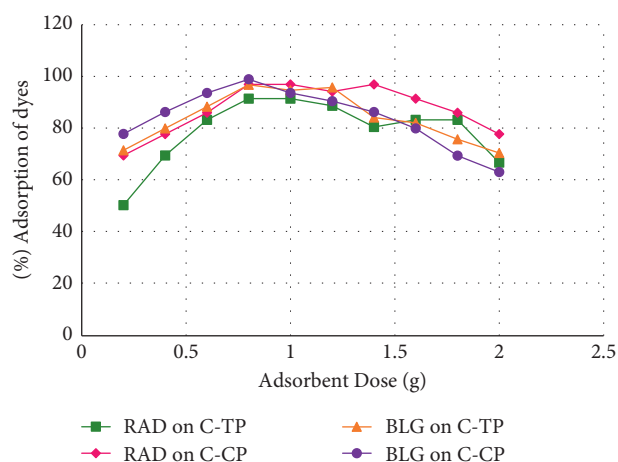


FIGURE 9: Effect of modified adsorbents dosage. Initial pH = 5, final pH for RAD on C-TP and C-CP = 4, BLG on C-TP = 4.5, and BLG on C-CP = 4.

from 60 to 70°C (75 to 77%). As a result, the optimal temperature of 30°C was determined for future experiments.

**3.3.5. Influence of pH on Adsorption.** The pH of the dye adsorption on lignocellulose substrates was adjusted using 0.1 M NaOH or 0.1 M HCl solutions during the experimental work [50]. The  $pH_{PZC}$  of both biosorbents TP and CP is significant for evaluating their adsorption potentials for both model dyes RAD and BLG and was experimentally determined to be 5.8 and 5.6 for TP and CP, respectively [24].

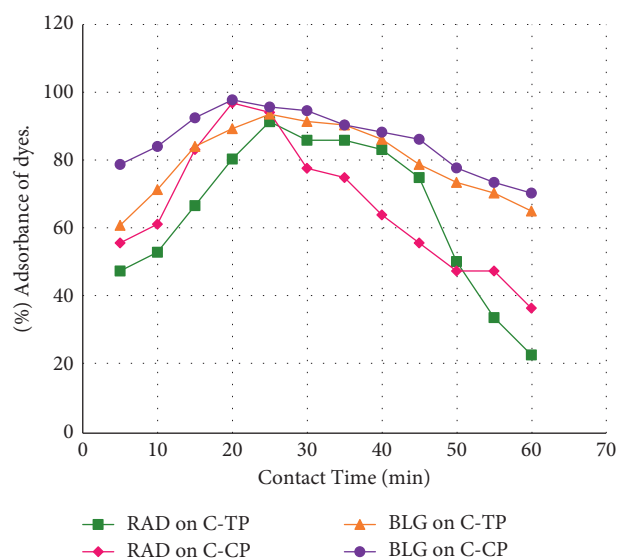


FIGURE 10: Contact time influence on adsorption. Initial pH = 5, final pH for RAD on C-TP and C-CP = 4, BLG on C-TP = 4.5, and BLG on C-CP = 4.

Figure 13 illustrates the influence of pH on the adsorption of model dyes RAD and BLG on citric acid-amended C-TP and C-CP in a pH range from 1 to 10. For this investigation, 25 ppm solutions with a volume of 25 mL were taken separately in four sets of Erlenmeyer flasks, and each set contained ten flasks for smooth experimental studies, while 0.8 g of each modified C-TP and C-CP was added to each pair of conical flasks containing 25 mL of RAD and BLG solutions with a



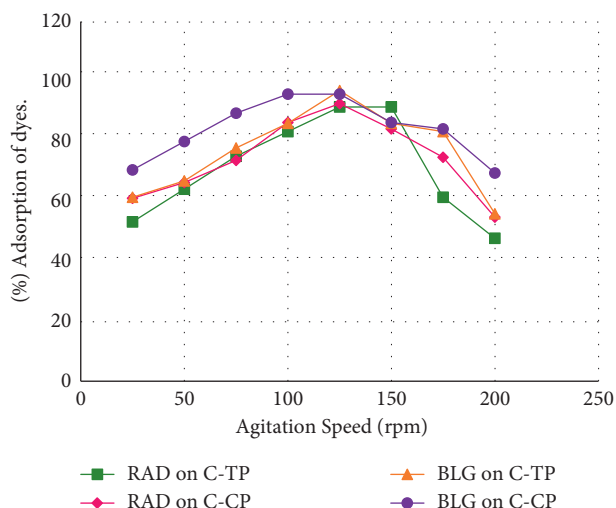


FIGURE 11: Effect of agitation speed on adsorption. Initial pH = 5, final pH for RAD on C-TP = 4, RAD on C-CP = 4.5, BLG on C-TP = 4.5, and BLG on C-CP = 4.

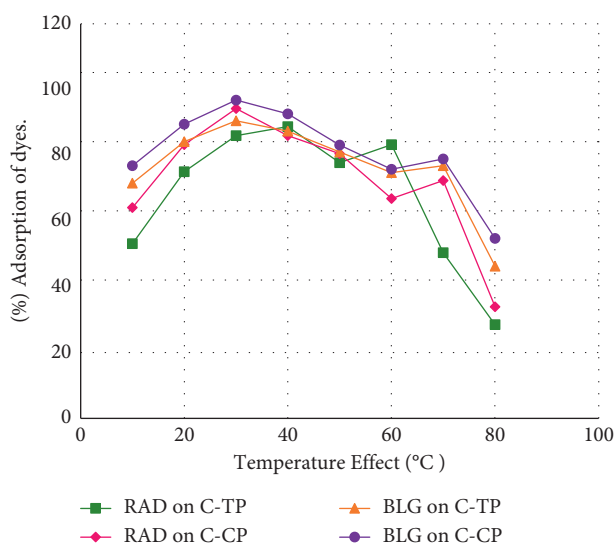


FIGURE 12: Influence of a change in temperature on biosorption. Initial pH = 5, final pH for RAD on C-TP and C-CP = 4, BLG on C-TP = 4.5, and BLG on C-CP = 4.

concentration of 25 ppm. The maximum adsorption elimination of RAD on C-TP was 96.99% at pH = 6, while RAD on C-CP was 91.51% at pH = 5, whereas maximum removal of BLG on C-TP was 93.68% and on C-CP it was 96.84% at pH 5, respectively. Figure 13 also illustrates that the decrease in adsorption performance of RAD and BLG was associated with an increase in pH, which influenced the development of equilibria with the adsorption binding active sites  $[\text{COO}^-]$  on the surfaces of biosorbents C-TP and C-CP and attractive associations of  $[\text{RAD}^+]$  and  $[\text{BLG}^+]$  cations with free  $[\text{OH}^-]$  ions in the aqueous solutions [51], resulting in hindering their accessibility to negatively charged adsorption sites on the interfaces of biosorbents [52].

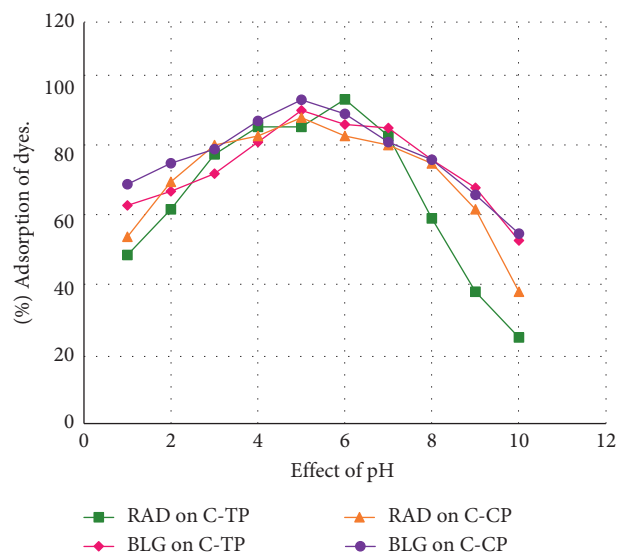


FIGURE 13: Influence of pH on adsorption mechanism.

Figure 13 also demonstrates that a decrease in pH causes the protonation of the negatively binding sites of biosorbents due to excessive  $\text{H}^+$  ions in the solution, which compete with the  $\text{RAD}^+$  and  $\text{BLG}^+$  cationic dye molecules, resulting in hindered adsorption at the interfaces of biosorbents [53]. Therefore, by considering the above results, an optimal pH value of 5 was determined for further studies.

### 3.4. Isothermal and Kinetic Modelling of Biosorption Processes

**3.4.1. Approach to Equilibrium Isothermal Models.** For the validity and reliability of the experiments conducted for the adsorption of RAD and BLG on citric acid-modified biosorbents (C-TP and C-CP), three equilibrium isothermal models by Langmuir, Freundlich, and Temkin were correlated and implemented by using linear equations (3), (6), and (7), respectively. The biosorption investigation was carried out with the following optimized parameters: The contact time interval was 20 minutes, the adsorbent dose utilized was 0.8 g of each of C-TP and C-CP, the temperature was  $30^\circ\text{C}$ , the agitation speed was 125 rpm, the initial pH of solutions used was 5, and the initial volume and concentrations of each dye solution (RAD and BLG) were 100 mL and 25 ppm.

(1) *Langmuir Isotherm.* Equation (3) displays a linear regression formulation of the Langmuir isotherm model [54], and Figure 14 elaborates on effective graphical factors.

$$\frac{1}{Q_e} = \left( \frac{1}{b \cdot Q_{\max}} \right) \frac{1}{C_e} + \left( \frac{1}{Q_{\max}} \right). \quad (3)$$

Here, quantity (ppm) of RAD and BLG adsorbed is indicated as " $Q_e$ ," while residual quantity is expressed as  $C_e$ , and the adsorption capability " $Q_{\max}$ " is the maximum adsorption capacity in  $\text{mg} \cdot \text{g}^{-1}$ , while " $b$ " is the adsorption capacity (L/g) [55].

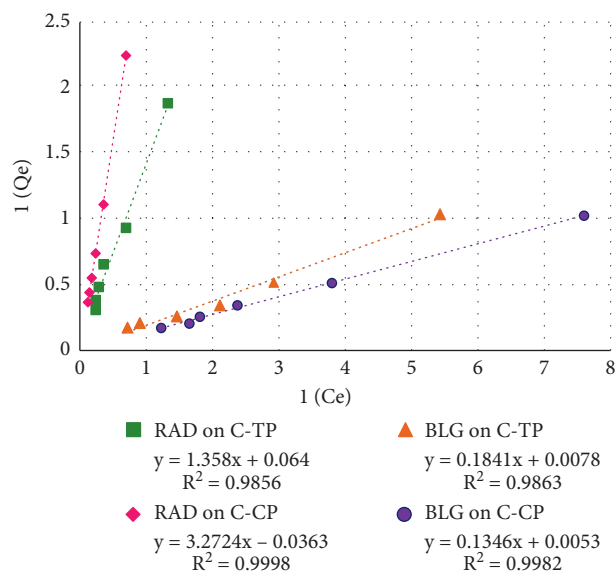


FIGURE 14: A comparison of the Langmuir isothermal model for the adsorptive dye removal efficiency of acid-treated biosorbents. Initial pH = 5, final pH for RAD on C-TP and C-CP = 4, BLG on C-TP = 4.5, and BLG on C-CP = 4.

The correlation coefficient ( $R^2$ ) for the adsorption of RAD on C-TP was 0.985, while on C-CP it was 0.999, whereas for the adsorption of BLG on C-TP it was 0.986 and on C-CP it was 0.999. The values of “ $R^2$ ” are close to unity in all cases, revealing that the Langmuir model is the best fit for the adsorption performance of C-TP and C-CP in this study. The maximum adsorption capacity ( $Q_{\max}$ ) for adsorption of RAD on C-TP was 15.6 and on C-CP it was 27.5 mg/g, whereas for BLG on C-TP it was 128 and on C-CP it was 189 mg/g, as tabulated in Table 3. The separation factor ( $R_L$ ) was calculated by using the following equation:

$$R_L = \left[ \frac{1}{1 + bC_o} \right]. \quad (4)$$

Its value between “0 and 1” reflects a good rate of adsorption. The separation factor ( $R_L$ ) for the adsorption of RAD on C-TP was 0.414 and on C-CP it was 0.750, whereas for the adsorption of BLG on C-TP it was 0.440 and on C-CP it was 0.458. These values, being less than “1,” indicate the good rate of adsorption and reflect the good and effective application of the Langmuir model for biosorption. Furthermore, the least values of RMSE for the adsorption of RAD on C-TP and C-CP were 2.76 and 2.03, respectively, while for BLG on C-TP and C-CP they were 4.1 and 5.2, respectively, indicating favorable adsorption for all cases. Moreover, “ $Q_{\max}$ ” values signify the monolayer homogeneity adsorption of dyes on C-TP and C-CP at a specific number of identical adsorption binding sites distributed on the interface boundaries of both biosorbents.

(2) *Freundlich Isothermal Model.* Freundlich isothermal model is employed to evaluate the surface heterogeneity of acid-modified adsorbents (C-TP and C-CP), as well as their activity for adsorption performance toward RAD and BLG

in aqueous solutions. It is concerned with the comparative distribution of energy in both physisorption and chemisorption. Equation (5) represents a linear trend of this isothermal system [54].

$$\ln q_e = \left( \ln K_F + \frac{1}{n} \ln C_e \right). \quad (5)$$

Here, “ $K_F$ ” ( $\text{mg}^{1-1/n} \text{L}^{1/n} \text{g}^{-1}$ ) is the binding factor and “ $n$ ” represents the adsorption frequency. A graphic comparison of the Freundlich model [ $\ln Q_e$  versus  $\ln C_e$ ] is depicted schematically in Figure 15, which illustrates straight lines for both citric acid-modified biosorbents (C-TP and C-CP).

As the graphical representation shown in Figure 15, for each model dye, exhibiting a slope ( $1/n$ ) less than 1 with correlation coefficient value for RAD on C-TP and C-CP was 0.94 and 0.91, respectively, whereas, for BLG on C-TP and C-CP was 0.77 and 0.92, respectively, which measured the interface diversity or uptake capacities of C-TP and C-CP. The correlation coefficients ( $R^2$ ) for the adsorptive removal of RAD on C-TP and C-CP were 0.96 and 0.93, respectively, whereas for BLG on C-TP and C-CP they were 0.98 and 0.94, respectively. The correlation coefficients, as tabulated in Table 3, reveal that the Langmuir model is more precise and perfect for this investigation than the Freundlich model.

(3) *Temkin Isothermal Studies.* Based on the fundamental assumption, Temkin modeling predicts an approximately equivalent dispersion of binding affinities on C-TP and C-CP. As a result, thermal diffusivity gradually decreases as the saturation of binding sites on the surface of adsorbents by RAD and BLG molecules increases. Linear representation of the Temkin isotherm is shown in the following equation:

$$q_e = (B_T \ln K_T + B_T \ln C_e). \quad (6)$$

The Temkin isotherm constant  $B_T = R_T/b_T$  ( $\text{kJmol}^{-1}$ ) designates the energy released during adsorption, whereas the equilibrium binding constant “ $K_T$ ” ( $\text{L.g}^{-1}$ ) reflects the maximal binding energy.

These constants were determined during the experimental research by linear regression of the graph plotted between “ $C_e$  and  $\ln C_e$ ” by using equation (6) for the adsorption of RAD and BLG on C-TP and C-CP, as shown graphically in Figure 16. The Temkin isotherm parameters are presented in Table 3, in which the heat of adsorption ( $B_T$ ) for RAD on C-TP and that on C-TP were 1.1512  $\text{Jmol}^{-1}$  and 1.315  $\text{Jmol}^{-1}$ , respectively, while for BLG on C-TP and on C-CP they were 1.28  $\text{Jmol}^{-1}$  and 1.5  $\text{Jmol}^{-1}$ , respectively. These  $B_T$  results are less than 8, confirming weak and physical adsorbate-adsorbent interactions and demonstrating physisorption rather than chemisorption.

The correlation coefficients ( $R^2$ ) as tabulated in Table 3 for adsorption of RAD on C-TP and C-CP were 0.83 and 0.93, respectively, whereas, for adsorption of BLG on C-TP and C-CP they were 0.95 and 0.84, respectively. These values of  $R^2$  for Temkin were less as compared to the Langmuir or Freundlich isothermal systems, suggesting that this model is unsatisfactorily fitted to this adsorption system. Equilibrium

TABLE 3: A comparison of isothermal parameters for the adsorptive elimination of RAD and BLG on citric acid-treated adsorbents C-TP and C-CP.

Parameters	RAD- C-TP	RAD-C-CP	BLG-C-TP	BLG-C-CP
Langmuir isothermal adsorption model				
$R^2$	0.986	0.985	0.99	0.998
$Q_{max}$ (mg/g)	15.625	27.55	128	189
$R_L$ (L/mg)	0.41428	0.75031	0.4403	0.4585
$b$ (L/mg)	0.047	0.011	0.04368	0.03938
Root mean sq. error	2.76	2.03	4.101	5.256
Freundlich isothermal adsorption model				
$R^2$	0.96	0.936	0.98	0.94
$1/n$	0.94	0.91	0.77	0.92
$n$ ( $1/m$ )	1.0675	1.0964	1.304	1.084
$K_F$ (mg/g)	1.4395	2.5656	2.9450	4.1133
Root mean sq. error	3.14	2.43	4.496	5.493
Temkin isothermal adsorption model				
$R^2$	0.831	0.939	0.95	0.84
$B_T$ ( $J.mol^{-1}$ )	1.1512	1.3154	1.28	1.5
$K_T$ ( $L.g^{-1}$ )	1.8228	1.0050	9.85	10.0

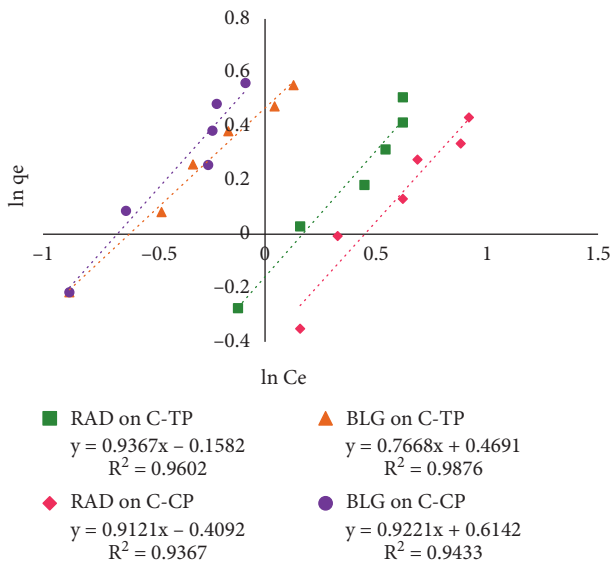


FIGURE 15: Evaluation of the Freundlich model regarding adsorptive dye removal efficiency of acid-treated biosorbents. Initial pH = 5, final pH for RAD on C-TP and C-CP = 4, BLG on C-TP = 4.5, and BLG on C-CP = 4.

binding constants " $K_T$ " ( $L.g^{-1}$ ) for adsorption of RAD on C-TP and C-CP were 1.822 and 1.00, respectively, while for BLG on C-TP and C-CP they were 9.85 and 10.0, respectively. The higher the magnitude of " $K_T$ ," the greater the number of accessible functional groups (like COOH, OH) on the surface of adsorbents [56]. The root mean square errors of C-TP and C-CP for adsorption of both RAD and BLG were determined by using equation (7) [57] and they are listed in Table 3.

$$RMSE = \sqrt{\sum \left[ \frac{(Q_{e(cal)} - Q_{e(exp)})^2}{N} \right]} \quad (7)$$

The smaller root mean square values suggest that the experimental findings for the adsorptive elimination of RAD and BLG on citric acid-treated adsorbents (C-TP and C-CP) were favorable.

3.4.2. *Batch Adsorption Kinetic Analyses.* Pseudo-first-order and pseudo-second-order kinetics have been used to investigate the adsorption of each dye (RAD and BLG) on chemically altered adsorbent materials (C-TP and C-CP) [58].

(1) *Pseudo-First-Order Kinetics.* Equation (8) displays the general formulation of Lagergren's expression for this kinetic [59].

$$\ln[Q_{eq} - Q_t] = [(\ln Q_{eq}) - (k_1 t)], \quad (8)$$

where " $Q_{eq}$ " (mg/g) is indeed the quantity of RAD and BLG taken at equilibrium and " $K_1$ " is the experimental data rate constant for pseudo-first-order kinetics ( $g/mg^{-1}min^{-1}$ ) and " $Q_t$ " (mg/g) is the adsorption capacity in "mg" of every dye RAD and BLG at time  $t$  ( $min^{-1}$ ) on 1 g of each C-TP and C-CP, respectively [60]. A plot " $\ln[Q_{eq} - Q_t]$  versus ( $t$ )" drawn illustrates adsorptive expulsion of both RAD and BLG on citric acid-modified biosorbents C-TP and C-CP, respectively, depicted in Figure 17. The corresponding characteristic parameters are shown in Table 4. The correlation coefficients  $R^2$  for adsorption of RAD on C-TP and C-CP were 0.53 and 0.71, respectively, while for adsorption of BLG on C-TP and C-CP they were 0.63 and 0.59, respectively. These smaller values of  $R^2$  for both dyes on each modified adsorbent reveal that Lagergren's expression for the pseudo-first-order mechanism presented in relation (8) is not properly applicable to the overall adsorption process. Furthermore, high values of RMSE for adsorption of RAD on C-TP and C-CP were 4.557 and 5.604, while for adsorption of BLG on C-TP and C-CP they were 6.15 and 10.272, also

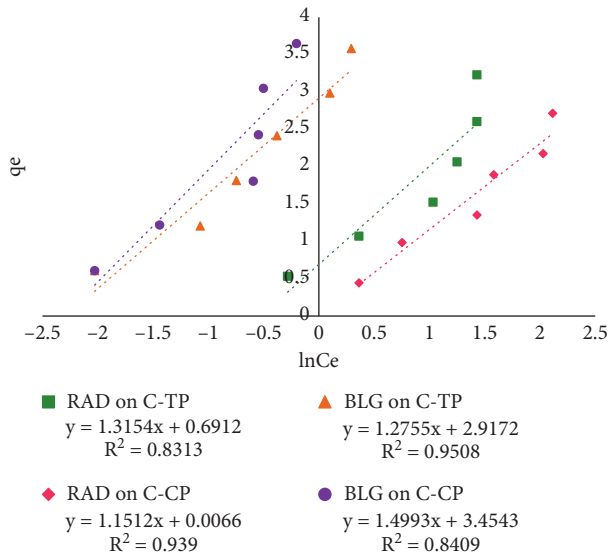


FIGURE 16: A comparison of the Temkin isothermal model for the adsorptive dye removal efficiency of acid-treated biosorbents. Initial pH = 5, final pH for RAD on C-TP and C-CP = 4, BLG on C-TP = 4.5, and BLG on C-CP = 4.

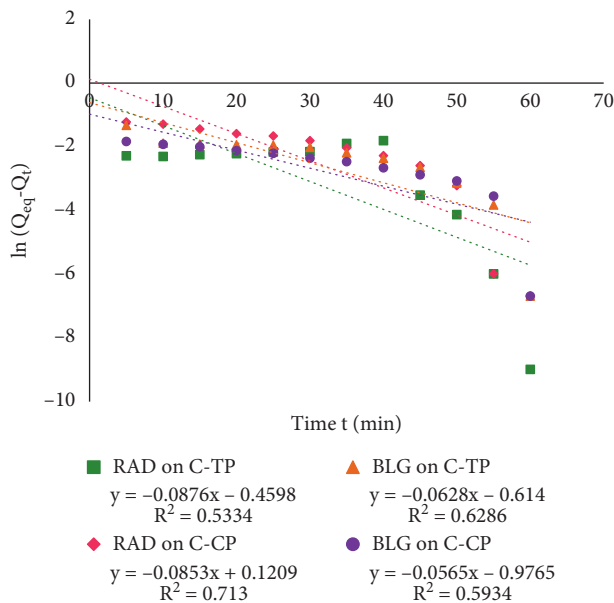


FIGURE 17: A comparative evaluation of the pseudo-first-order kinetics for the adsorptive dye removal performance of acid-treated biosorbents. Initial pH = 5, final pH for RAD on C-TP and C-CP = 4, BLG on C-TP = 4.5, and BLG on C-CP = 4. (b) Pseudo-second-order kinetics.

indicating that this kinetic model is not suitable and does not fit this adsorption system.

The rate equation (9) for pseudo-second-order mechanism was presented by HO and McKay and is given as follows [61]:

$$\frac{t}{Q_t} = \left[ \left( \frac{1}{K_2 \cdot Q_{eq}^2} \right) + \left( \frac{t}{Q_{eq}} \right) \right]. \quad (9)$$

In the above equation,  $Q_{eq}$  (mg/g) denotes the optimum adsorption capability, whereas  $Q_t$  signifies the adsorption efficiency in time  $t$  ( $\text{min}^{-1}$ ). An experimental data rate factor ( $\text{g}/\text{mg}^{-1}\text{min}^{-1}$ ) is termed as  $K_2$  [62].

The correlational evaluation for graph plotted linearly among ( $Q_t$  vs  $t$ ), depicted graphically displayed in Figure 18. This data is used to determine the rate constants and adsorption capability from the slope by using equation (9). The significant parameters have been determined and are listed in Table 4. The correlation coefficients ( $R^2$ ) for the adsorption of RAD on C-TP and C-CP were 0.92 and 0.96, respectively, while for the adsorption of BLG on C-TP and C-CP they were 0.96 and 0.99, respectively, near to unity, indicating that the pseudo-second-order kinetic model seems to be more fit than the pseudo-first-order kinetic model. The RMSE values of pseudo-second-order kinetics for the adsorption of RAD on C-TP and C-CP were 3.328 and 3.418, respectively, while for the adsorption of BLG on C-TP and C-CP they were 4.5 and 6.63, as mentioned in Table 4. These values are smaller rather pseudo second order kinetic. This also reflects the suitability and fitness of the pseudo-second-order model for this adsorption system.

(2) *Determination of Percent Relative Deviation (P)*. The percent relative deviation has been used to determine the validity of kinetics models for the adsorption of RAD and BLG on both C-TP and C-CP. Equation (10) was employed to determine it, and the conclusions are summed up in Table 4. The least values of percent relative deviation for the adsorption of RAD on C-TP and C-CP were  $-0.551$  and  $-1.186$ , while for BLG on C-TP and C-CP they were  $-0.553$  and  $-0.103$ , respectively, reflecting that second-order kinetics support the acceptability and suitability in better way as compared to the first-order kinetics [63].

$$\% \text{Relative Deviation (P)} = \frac{100}{N} \sum \left[ \frac{(Q_{e(\text{exp})} - Q_{e(\text{cal})})}{Q_{e(\text{exp})}} \right], \quad (10)$$

where  $N$  represents the number of observations,  $Q_e$  (exp.) (mg/g) denotes the experimental value of adsorption binding capacity, and  $Q_e$  (cal.) (mg/g) represents the calculated value of adsorption binding capabilities.

(3) *Thermodynamic Investigation*. Temperature change will have an impact on the adsorption mechanism, leading to variations in the kinetic energies of RAD and BLG molecules. Because of the entire porous interface of used cellulosic biomass, this factor accelerates the amount of dispersion of RAD and BLG. Table 5 highlights that the effectiveness and rate of adsorption of RAD and BLG on innovative C-TP and C-CP are determined by operational thermodynamic parameters, such as Gibbs free energy, enthalpy changes, and entropy changes. The increase ( $-\Delta G^\circ$ )



TABLE 4: A comparison of parameters for kinetics studies.

Parameters	Kinetic equilibrium models for adsorption			
	RAD-C-TP	RAD-C-CP	BLG-C-TP	BLG-C-CP
Evaluation of pseudo-first-order kinetics				
$R^2$	0.53	0.71	0.63	0.59
$Q_e$ (exp.-mg/g)	0.46	0.62	0.50	0.75
$Q_e$ (cal.-mg/g)	0.63	1.13	0.54	0.38
$K_1$ (g/mg <sup>-1</sup> min <sup>-1</sup> )	0.00146	-0.00142	-0.00105	-0.00094
Root mean sq. error	4.557	5.604	6.157	10.272
% relative deviation	-2.837	-6.359	2.05	3.82
Evaluation of pseudo-second-order kinetics				
$R^2$	0.922	0.963	0.963	0.994
$K_2$ (g/mg <sup>-1</sup> min <sup>-1</sup> )	0.275	0.11	0.201	0.369
$Q_e$ (exp.mg/g)	0.46	0.62	0.50	0.75
$Q_e$ (cal.mg/g)	0.494	0.712	0.54	0.76
Root mean sq. error	3.328	3.418	4.502	6.637
% relative deviation	-0.551	-1.186	-0.553	-0.103

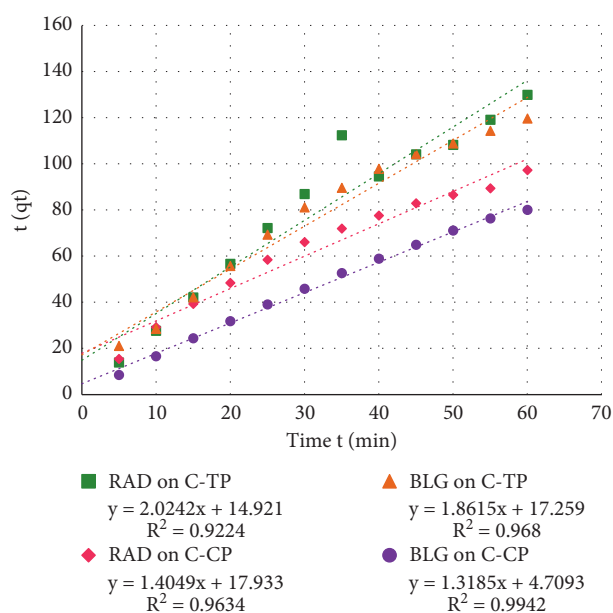


FIGURE 18: A comparison of the pseudo-second-order kinetics for the adsorptive dye removal performance of acid-treated biosorbents. Initial pH = 5, final pH for RAD on C-TP and C-CP = 4, BLG on C-TP = 4.5, and BLG on C-CP = 4.

of both unique citric acid-treated adsorbents reflects a rapid, exothermic, and spontaneous adsorption mechanism. These calculations were estimated from the following equation:

$$\Delta G^\circ = [RT(\ln K_D)], \quad (11)$$

where “ $R$ ” is the universal gas constant, “ $T$ ” is temperature in Kelvin, and  $K_D$  (distribution coefficient) is determined using the following equation:

$$K_D = \frac{(C_o - C_e)}{C_e}. \quad (12)$$

Enthalpy change values varying from 2.1 to 20.9 kJmol<sup>-1</sup> suggest physisorption, whereas values ranging from 80 to

200 kJmol<sup>-1</sup> reflect strong interactions leading to chemisorption. Adsorption of each RAD and BLG on C-TP and C-CP was observed chemically in nature and summarized in Table 5. The fact that the citric acid-altered adsorbents have greater enthalpy change values, determined from equation (13), promotes adsorption over their untreated forms.

The distortedness at the solid-liquid boundaries during the adsorption can also be determined by the change in entropy ( $\Delta S^\circ$ ) and was calculated as follows:

$$\ln K_D = \left[ \frac{\Delta S^\circ}{R} - \frac{\Delta H^\circ}{RT} \right]. \quad (13)$$

Its high positive values favor a considerable pace of adsorption [64]. A linear graph was drawn across “ $\ln K_D$  versus  $1/T$ ,” depicted in Figure 19.

The slope and intercept were used to determine the values of  $\Delta H^\circ$  and  $\Delta S^\circ$  for the adsorptive elimination of dyes (RAD and BLG) on C-TP and C-CP. Equation (14), which is a rearranged form of equation (13), can be used to determine  $\Delta H^\circ$  and  $\Delta S^\circ$ .

$$\Delta G^\circ = [\Delta H^\circ - T\Delta S^\circ]. \quad (14)$$

The energy of activation ( $E_a$ ) for the adsorptive elimination of each RAD and BLG on C-TP and C-CP was calculated using the Arrhenius equation.

$$\ln K = \left[ \ln A - \left( \frac{E_a}{RT} \right) \right]. \quad (15)$$

Physical adsorption,  $E_a$ , ranges from 5 to 40 kJ/mole, whereas chemical adsorption ranges from 40 to 800 kJ/mole. In this investigation, the data given in Table 5 reveals the physisorption process.

**3.5. Mechanism of Adsorption.** As evidenced by FT-IR and SEM analysis, chemically modified adsorbents C-TP and C-CP with chelator (citric acid) were suggested to include various additional moieties, including carboxylic acids and hydroxyl, carbonyls, and primary amines across their

TABLE 5: Thermodynamic comparative evaluation of the adsorptive elimination of RAD and BLG by citric acid-treated adsorbents (C-TP and C-CP).

Thermodynamic parameters analysis					
Temperature	$K_D$	$\Delta G^0$ (kJmol <sup>-1</sup> )	$\Delta H^0$ (kJmol <sup>-1</sup> )	$\Delta S^0$ (Jmol <sup>-1</sup> K <sup>-1</sup> )	$E_a$ (kJmol <sup>-1</sup> )
RAD on C-TP					
298 K	2.614	-2.4	-44	154	44
308 K	4.141	-3.7			
318 K	7.902	-5.5			
RAD on C-CP					
298 K	3.506	-3.1	-61	213	61
308 K	6.157	-4.7			
318 K	16.38	-7.4			
BLG on C-TP					
298 K	1.969	-1.7	-67	228	67
308 K	3.703	-3.4			
318 K	10.728	-6.3			
BLG on C-CP					
298 K	2.006	-1.7	-73	249	73
308 K	4.08	-3.6			
318 K	12.768	-6.7			

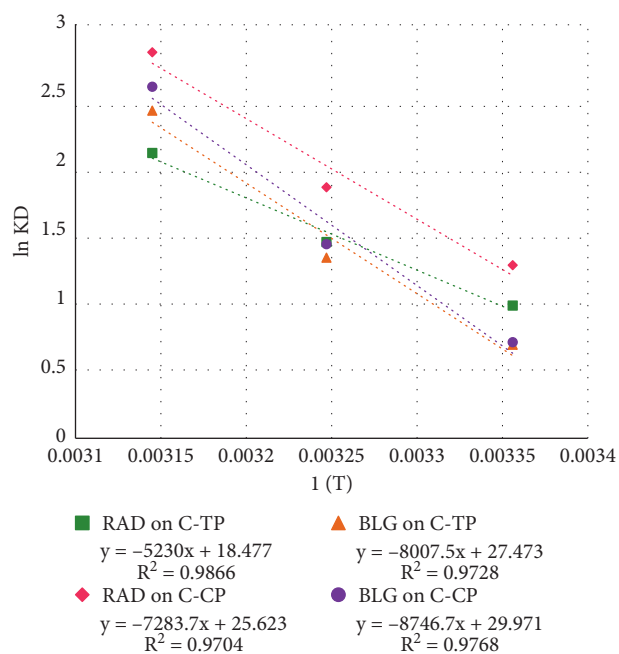


FIGURE 19: A comparison of the thermodynamics parameters for the adsorptive dye removal performance of acid-treated biosorbents. Initial pH = 5, final pH for RAD on C-TP and C-CP = 4, BLG on C-TP = 4.5, and BLG on C-CP = 4.

interfacing regions to interact with RAD and BLG, and they were also discussed and explored in Sections 2.4 and 3.1. A schematic and proposed interaction mechanisms created by C-TP and C-CP with dye molecules (RAD and BLG) can be seen in Figure 20. The weak Van der Waals interactions, such as hydrogen bonding [65], surface complexation [66], chelation [67], ion exchange [68], and electrostatic forces [69], cause chemical bonding between dye molecules (RAD and BLG) on chemically amended-adsorbent surfaces.

According to reported data, chemical modification by using organic acids like citric acid, tartaric acid, or oxalic acids on solid base adsorbents alters and improves their surface morphology, orientation, and topography by providing additional functional groups like COOH and OH, resulting in improved adsorption capacity and affinity of novel C-TP and C-CP lignocellulosic biomass. It was noted that the adsorption phenomenon was highly dependent on pH of the dye solutions. The rate of adsorption was increased and directly related to the ionization of carboxylic acid, with the result of producing negatively charged adsorption sites at the interface of C-TP and C-CP. The deprotonation of carboxylic acids was associated with the rise in pH. The resulting ion exchange mechanism of H<sup>+</sup> with cations of RAD<sup>+</sup> and BLG<sup>+</sup> was carried out as shown in Figure 20 [47, 70].

In addition to this, hydrogen bonding linkages in between "OH" moieties on lignocellulosic biomass of C-TP and C-CP and a lone pair on nitrogen of amino groups of both RAD and BLG were created, which partially contributed to enhancing the rate of adsorption [47].

Furthermore, electrostatic forces were also established between cations of dye molecules and negatively active binding sites on the surfaces of both modified adsorbents [70]. Under the influence of such associations [51, 71], mentioned below in Figure 21, the adsorption of hazardous and toxic dyes has become more efficient and quicker during this experimental approach.

**3.6. Conclusion.** In this investigation, the peels of *Trapa natans* and *Citrullus lanatus* were pretreated chemically with tricarboxylic acid (citric acid) to provide modified and effective novel forms for the adsorptive removal of harmful, noxious, and carcinogenic basic and cationic dyes like Rhodamine B and Brilliant Green from the aqueous system. FT-IR and SEM analysis have provided evidence for

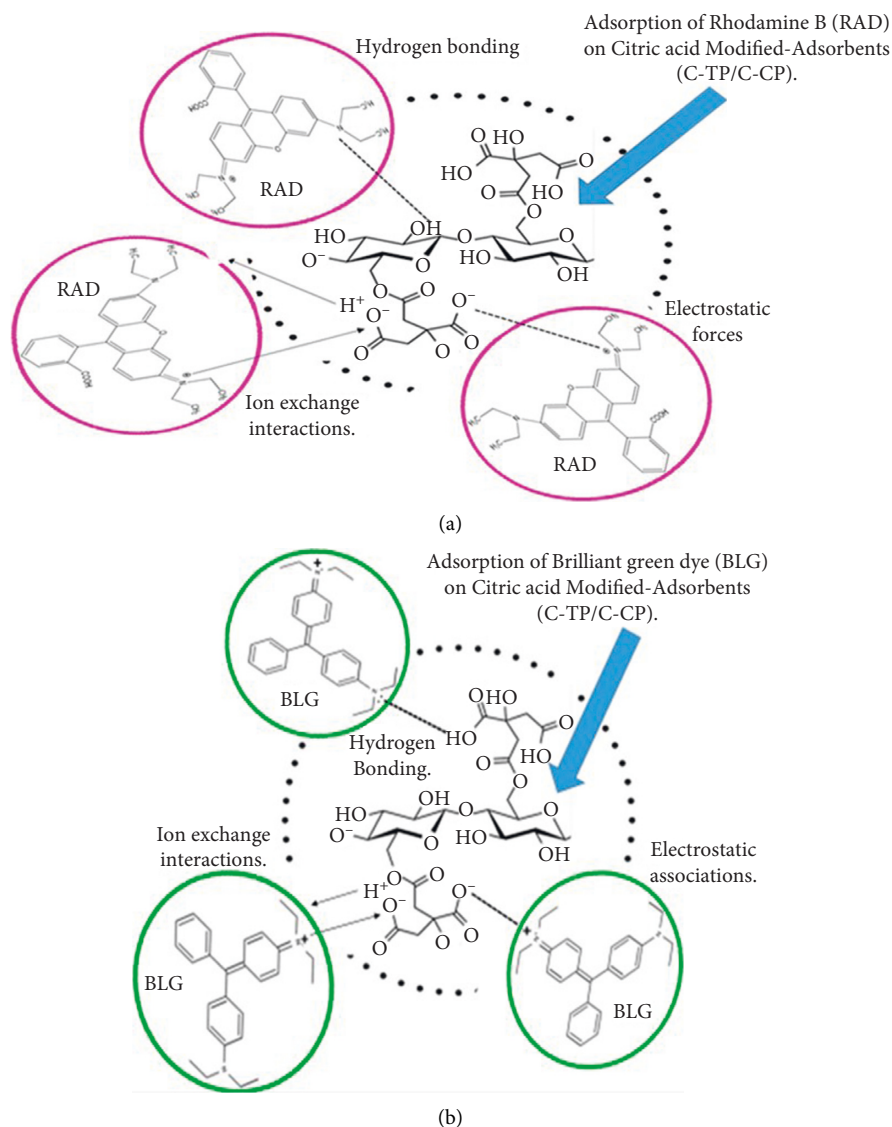


FIGURE 20: Schematic diagram for the adsorption mechanism. (a) RAD on C-TP and C-CP. (b) BLG on C-TP and C-CP.

alteration of surface amendment under the influence of the extra and additional oxygen-containing groups like COOH and OH, which are directly associated with enhancing the adsorption efficiency. Langmuir isotherm has shown that the maximum adsorption capacity ( $Q_{max}$ ) for RAD on C-TP was 15.6 and that on C-CP was 27.5 mg/g, while for BLG on C-TP it was 128 and on C-CP it was 189 mg/g. Furthermore, correlation coefficient ( $R^2$ ) for the adsorption of RAD on C-TP was 0.985, while on C-CP it was 0.999, whereas for the adsorption of BLG on C-TP it was 0.986 and on C-CP it was 0.999. Therefore, " $R^2$ " is close to unity in all cases, revealing that the Langmuir model is the best fit for the adsorption performance of C-TP and C-CP in this study rather than the Freundlich and Temkin isotherms. High Langmuir isotherm regression coefficients, on the other hand, indicate that the adsorption mechanism is monolayer, with homogeneous chemisorption on equivalent active binding sites that are abundant on the surfaces of acid-treated biosorbents (C-TP

and C-CP). The heats of adsorption ( $B_T$ ) for RAD on C-TP and on C-CP were 1.1512 Jmol<sup>-1</sup> and 1.315 Jmol<sup>-1</sup>, respectively, whereas  $B_T$  for BLG on C-TP and on C-CP was 1.28 Jmol<sup>-1</sup> and 1.5 Jmol<sup>-1</sup>, respectively, indicating weak and physical adsorbate-adsorbent interactions and demonstrating physisorption rather than chemisorption. The correlation coefficients ( $R^2$ ) for the adsorption of RAD on C-TP and C-CP were 0.92 and 0.96, respectively, while for the adsorption of BLG on C-TP and C-CP they were 0.96 and 0.99, respectively, near to unity, indicating that the pseudo-second-order kinetic model seems to be more fit than the pseudo-first-order kinetic model. High negative  $\Delta G^0$  predicts that the adsorption mechanism is exothermic as well as spontaneous. The adsorption efficiency of the citric acid-treated peels of *Trapa natans* and *Citrullus lanatus* was also assessed by comparing them with the adsorption ability of previously reported biosorbents, as illustrated in Table 2, and it was concluded that these novel adsorbents have a

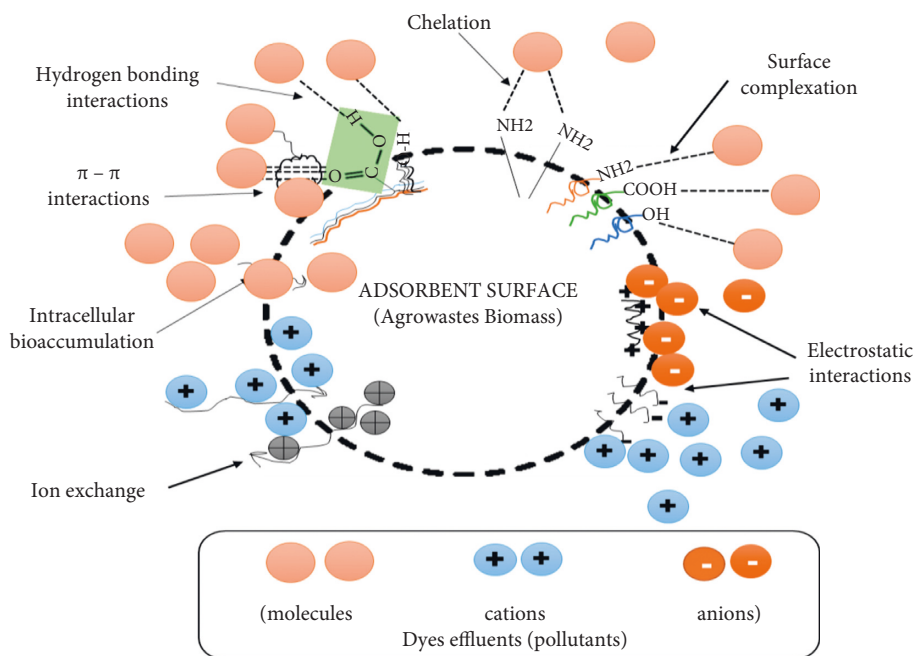


FIGURE 21: Proposed adsorption interactions between adsorbate and adsorbents are depicted schematically.

much higher ability to eliminate and evacuate basic and cationic dyes like Rhodamine B and Brilliant Green from wastewater [72].

## Abbreviations

TP:	Raw <i>Trapa natans</i> peels
CP:	Raw <i>Citrullus lanatus</i> peels
C-TP:	Citric acid-treated <i>Trapa natans</i> peels
C-CP:	Citric acid-treated <i>Citrullus lanatus</i> peels
RAD:	Rhodamine B dye
BLG:	Brilliant Green Dye
FT-IR:	Fourier-transform infrared spectroscopy
SEM:	Scanning electron microscopy
pH <sub>PZC</sub> :	Point of zero charge
RMSE:	Root mean square errors.
P:	Percent relative deviation

## Data Availability

All data related to this work are presented in Results and Discussion section along with references.

## Conflicts of Interest

Regarding the publication of this article, the authors have no potential conflicts of interest.

## Acknowledgments

The authors appreciate the sample analysis services provided by LUMS and COMSAT Lahore. The authors are thankful to home department for funding this work.

## References

- [1] S. Gita, A. Hussan, and T. Choudhury, "Impact of textile dyes waste on aquatic environments and its treatment," *Environment and Ecology*, vol. 35, no. 3C, pp. 2349–2353, 2017.
- [2] J. Mittal, V. Thakur, and A. Mittal, "Batch removal of hazardous azo dye Bismark Brown R using waste material hen feather," *Ecological Engineering*, vol. 60, pp. 249–253, 2013.
- [3] R. A. E.-G. Mansour, M. G. Simeida, and A. A. Zaatout, "Removal of brilliant green dye from synthetic wastewater under batch mode using chemically activated date pit carbon," *RSC Advances*, vol. 11, no. 14, pp. 7851–7861, 2021.
- [4] R. Kant, "Textile dyeing industry an environmental hazard," *Natural Science*, vol. 4, no. 1, pp. 22–26, 2012.
- [5] R. Rehman, S. J. Muhammad, and M. Arshad, "Brilliant green and acid orange 74 dyes removal from water by *Pinus roxburghii* leaves in naturally benign way: an application of green chemistry," *Journal of Chemistry*, vol. 2019, Article ID 3573704, 10 pages, 2019.
- [6] R. D. Saini, "Textile organic dyes: polluting effects and elimination methods from textile waste water," *International Journal of Chemical Engineering Research*, vol. 9, no. 1, pp. 121–136, 2017.
- [7] S. Haq, A. W. Raja, S. U. Rehman et al., "Phytogenic synthesis and characterization of NiO-ZnO nanocomposite for the photodegradation of brilliant green and 4-nitrophenol," *Journal of Chemistry*, vol. 2021, Article ID 3475036, 10 pages, 2021.
- [8] B. Cojocariu, A. M. Mocanu, G. Nacu, and L. Bulgariu, "Possible utilization of PET waste as adsorbent for Orange G dye removal from aqueous media," *Desalination and Water Treatment*, vol. 104, pp. 338–345, 2018.
- [9] L. Bulgariu, L. B. Escudero, O. S. Bello et al., "The utilization of leaf-based adsorbents for dyes removal: a review," *Journal of Molecular Liquids*, vol. 276, pp. 728–747, 2019.



- [10] D. Shrestha, "Efficiency of wood-dust of *Dalbergia sisoo* as low-cost adsorbent for rhodamine-B dye removal," *Nanomaterials*, vol. 11, no. 9, Article ID 2217, 2021.
- [11] R. Ghibate, O. Senhaji, and R. Taouil, "Kinetic and thermodynamic approaches on Rhodamine B adsorption onto pomegranate peel," *Case Studies in Chemical and Environmental Engineering*, vol. 3, Article ID 100078, 2021.
- [12] T. Utheyakumaran, *Removal of Rhodamine B Dye in Aqueous Solution Using Raw Timber Wood Sawdust as Adsorbent*, Universiti Malaysia Kelantan, Kota Bharu, Malaysia, 2020.
- [13] M. Gören, "Removal of rhodamine B from aqueous solution by using pine cone activated with  $\text{HNO}_3$ ," *Journal of International Environmental Application & Science*, vol. 16, no. 3, pp. 123–132, 2021.
- [14] S. Singh, N. Parveen, and H. Gupta, "Adsorptive decontamination of rhodamine-B from water using banana peel powder: a biosorbent," *Environmental Technology & Innovation*, vol. 12, pp. 189–195, 2018.
- [15] B. S. Inbaraj and N. Sulochana, "Use of jackfruit peel carbon (JPC) for adsorption of rhodamine-B, a basic dye from aqueous solution," *Indian Journal of Chemical Technology*, vol. 13, pp. 17–23, 2006.
- [16] K. Sukla Baidya and U. Kumar, "Adsorption of brilliant green dye from aqueous solution onto chemically modified areca nut husk," *South African Journal of Chemical Engineering*, vol. 35, pp. 33–43, 2021.
- [17] N. Buvaneswari, "Removal of brilliant green dye by the adsorption on *Sesamum indicum* tree waste from aqueous solution and its recovery," *Journal of Engineering Sciences*, vol. 11, no. 3, 2020.
- [18] R. A. Mansour, A. El Shahawy, A. Attia, and M. S. Beheary, "Brilliant green dye biosorption using activated carbon derived from guava tree wood," *International Journal of Chemical Engineering*, vol. 2020, Article ID 8053828, 12 pages, 2020.
- [19] S. Sawasdee, H. Jankerd, and P. Watcharabundit, "Adsorption of dyestuff in household-scale dyeing onto rice husk," *Energy Procedia*, vol. 138, pp. 1159–1164, 2017.
- [20] R. C. Pundlik, S. D. Chowdhury, R. R. Dash, and P. Bhunia, "Life-cycle assessment of agricultural waste-based and biomass-based adsorbents," *Biomass, Biofuels, Biochemicals*, pp. 669–695, Elsevier Science, Amsterdam, Netherlands, 2021.
- [21] S. Latif, R. Rehman, M. Imran, S. Iqbal, A. Kanwal, and L. Mitu, "Removal of acidic dyes from aqueous media using *Citrullus lanatus* peels: an agrowaste-based adsorbent for environmental safety," *Journal of Chemistry*, vol. 2019, Article ID 6704953, 9 pages, 2019.
- [22] O. H. Heba, S. Ali, and N. Abdullah, "Chelate coupling with pineapple leaves as a modified bio-sorbent for lead ions (II) removal," *International journal of Environmental Science and Technology*, vol. 16, no. 11, pp. 7293–7304, 2019.
- [23] Y. Zhao, H. Yang, J. Sun, Y. Zhang, and S. Xia, "Enhanced adsorption of Rhodamine B on modified oil-based drill cutting ash: characterization, adsorption kinetics, and adsorption isotherm," *ACS Omega*, vol. 6, no. 26, pp. 17086–17094, 2021.
- [24] M. S. Hussain, R. Rehman, and M. Imran, "Isothermal and kinetic investigation of exploring the potential of citric acid-treated *Trapa natans* and *Citrullus lanatus* peels for biosorptive removal of brilliant green dye from water," *Journal of Chemistry*, vol. 2021, Article ID 6051116, 23 pages, 2021.
- [25] R. Rehman, J. Anwar, T. Mahmud, and M. Salman, "Removal of murexide (dye) from aqueous media using rice husk as an adsorbent," *Journal of the Chemical Society of Pakistan*, vol. 33, no. 4, p. 598, 2011.
- [26] V. Vaishnav, S. Chandra, and K. Daga, "Adsorption studies of Zn (II) ions from wastewater using *calotropis procera* as an adsorbent," *Research Journal of Recent Sciences*, vol. 1, pp. 160–165, 2012.
- [27] Y. Hua, J. Xiao, Q. Zhang, C. Cui, and C. Wang, "Facile synthesis of surface-functionalized magnetic nanocomposites for effectively selective adsorption of cationic dyes," *Nanoscale Research Letters*, vol. 13, no. 1, p. 99, 2018.
- [28] N. I. Taib, N. A. Rosli, N. I. Saharrudin, N. M. Rozi, N. A. A. Kasdiehram, and N. N. T. Abu Nazri, "Kinetic, equilibrium, and thermodynamic studies of untreated watermelon peels for removal of copper (II) from aqueous solution," *Desalination and Water Treatment*, vol. 227, pp. 289–299, 2021.
- [29] P. Saravanan, J. Josephraj, B. Pushpa Thillainayagam, and G. Ravindiran, "Evaluation of the adsorptive removal of cationic dyes by greening biochar derived from agricultural bio-waste of rice husk," *Biomass Conversion and Biorefinery*, pp. 1–14, 2021.
- [30] F. Ngugi, "Adsorption of rhodamine b from aqueous solution using mangroves (*Rhizophora mucronata*) carbon nanotubes nanocomposites," *International Journal of Multidisciplinary Research and Development*.
- [31] A. Selvakumar and S. Rangabhashiyam, "Biosorption of Rhodamine B onto novel biosorbents from *Kappaphycus alvarezii*, *Gracilaria salicornia* and *Gracilaria edulis*," *Environmental Pollution*, vol. 255, Article ID 113291, 2019.
- [32] R. J. Nascimento, K. R. A. Pereira, and F. Avelino, "Parametric and modeling studies of Rhodamine-B adsorption using coconut coir-based materials as eco-friendly adsorbents," *Journal of Environmental Chemical Engineering*, vol. 9, no. 5, Article ID 105943, 2021.
- [33] M. R. R. Kooh, M. K. Dahri, and L. B. Lim, "Jackfruit seed as a sustainable adsorbent for the removal of Rhodamine B dye," *Journal of Environment & Biotechnology Research*, vol. 4, no. 1, pp. 7–16, 2016.
- [34] Q. Li, X. Tang, Y. Sun et al., "Removal of Rhodamine B from wastewater by modified *Volvariella volvacea*: batch and column study," *RSC Advances*, vol. 5, no. 32, pp. 25337–25347, 2015.
- [35] X. Guo, Z. Liu, Z. Tong, N. Jiang, and W. Chen, "Adsorption of rhodamine B from an aqueous solution by acrylic-acid-modified walnut shells: characterization, kinetics, and thermodynamics," *Environmental Technology*, pp. 1–25, 2021.
- [36] F. H. M. Souza, V. F. C. Leme, G. O. B. Costa, K. C. Castro, T. R. Giraldo, and G. S. S. Andrade, "Biosorption of rhodamine B using a low-cost biosorbent prepared from inactivated *Aspergillus oryzae* cells: kinetic, equilibrium and thermodynamic studies," *Water, Air, & Soil Pollution*, vol. 231, no. 5, pp. 242–313, 2020.
- [37] L. L. Zhi and M. A. A. Zaini, "Rhodamine B dyes adsorption on palm kernel shell based activated carbons," *Malaysian Journal of Fundamental and Applied Sciences*, vol. 15, pp. 743–747, 2019.
- [38] A. Aadil, S. Murtaza, K. Shahid, M. Munir, R. Ayub, and S. Akber, "Comparative study of adsorptive removal of Congo red and brilliant green dyes from water using peanut shell," *Middle-East Journal of Scientific Research*, vol. 11, no. 6, pp. 828–832, 2012.
- [39] R. Rehman, B. Salariya, and L. Mitu, "Batch scale adsorptive removal of brilliant green dye using *Trapa natans* peels in cost

- effective manner,” *Revue Chimique*, vol. 67, pp. 1333–1337, 2016.
- [40] A. A. Romzi, M. R. R. Kooh, L. B. L. Lim, N. Priyantha, and C. M. Chan, “Environmentally friendly adsorbent derived from rock melon skin for effective removal of toxic brilliant green dye: linear versus non-linear analyses,” *International Journal of Environmental Analytical Chemistry*, pp. 1–20, 2021.
- [41] L. T. Popoola, T. A. Aderibigbe, A. S. Yusuff, and M. M. Munir, “Brilliant green dye adsorption onto composite snail shell–rice husk: adsorption isotherm, kinetic, mechanistic, and thermodynamics analysis,” *Environmental Quality Management*, vol. 28, no. 2, pp. 63–78, 2018.
- [42] M. P. Tavlieva, S. D. Genieva, V. G. Georgieva, and L. T. Vlaev, “Kinetic study of brilliant green adsorption from aqueous solution onto white rice husk ash,” *Journal of Colloid and Interface Science*, vol. 409, pp. 112–122, 2013.
- [43] F. de Castro Silva, M. M. F. da Silva, L. C. B. Lima, J. A. Osajima, and E. C. da Silva Filho, “Modifying cellulose with metaphosphoric acid and its efficiency in removing brilliant green dye,” *International Journal of Biological Macromolecules*, vol. 114, pp. 470–478, 2018.
- [44] Z. N. Abudi, F. Lattieff, T. Fahem, and M. Nsaif Abbas, “Isotherm and kinetic study of the adsorption of different dyes from aqueous solution using banana peel by two different methods,” *Global Journal of Bio-Science and Biotechnology*, vol. 7, no. 2, pp. 220–229, 2018.
- [45] A. Sharafzad, S. Tamjidi, and H. Esmaeili, “Calcined lotus leaf as a low-cost and highly efficient biosorbent for removal of methyl violet dye from aqueous media,” *International Journal of Environmental Analytical Chemistry*, vol. 101, no. 15, pp. 2761–2784, 2021.
- [46] A. Nasrullah, H. Khan, A. S. Khan et al., “Potential biosorbent derived from *Calligonum polygonoides* for removal of methylene blue dye from aqueous solution,” *The Scientific World Journal*, vol. 2015, Article ID 562693, 11 pages, 2015.
- [47] K. Roa, E. Oyarce, A. Boulett et al., “Lignocellulose-based materials and their application in the removal of dyes from water: a review,” *Sustainable Materials and Technologies*, vol. 29, Article ID e00320, 2021.
- [48] M. Mohapi, J. S. Sefadi, M. J. Mochane, S. I. Magagula, and K. Lebelo, “Effect of LDHs and other clays on polymer composite in adsorptive removal of contaminants: a review,” *Crystals*, vol. 10, no. 11, p. 957, 2020.
- [49] E. P. Fernandes, T. S. Silva, C. M. Carvalho et al., “Efficient adsorption of dyes by  $\gamma$ -alumina synthesized from aluminum wastes: kinetics, isotherms, thermodynamics and toxicity assessment,” *Journal of Environmental Chemical Engineering*, vol. 9, no. 5, Article ID 106198, 2021.
- [50] G. A. Tochetto, T. C. da Silva, J. Bampi, C. da Luz, G. D. Leal Pasquali, and A. Dervanoski, “Highly efficient biosorbent produced from *Syagrus romanzoffiana* to be applied in water treatment,” 2021.
- [51] H. Khalili, A. Ebrahimi Pirbazari, F. Esmaeili Khalil Saraei, and S. H. Mousavi, “Simultaneous removal of basic dyes from binary systems by modified orange peel and modeling the process by an intelligent tool,” *Preprints*, Article ID 2021060224, 2021.
- [52] F. Largo, R. Haounati, S. Akhouairi et al., “Adsorptive removal of both cationic and anionic dyes by using sepiolite clay mineral as adsorbent: experimental and molecular dynamic simulation studies,” *Journal of Molecular Liquids*, vol. 318, Article ID 114247, 2020.
- [53] M. Rabipour, Z. Sekhvat Pour, R. Sahraei, M. Ghaemy, M. Erfani Jazi, and T. E. Mlsna, “pH-sensitive nanocomposite hydrogels based on poly (vinyl alcohol) macromonomer and graphene oxide for removal of cationic dyes from aqueous solutions,” *Journal of Polymers and the Environment*, vol. 28, no. 2, pp. 584–597, 2020.
- [54] Ü. Geçgel, G. Özcan, and G. Ç. Gürpınar, “Removal of methylene blue from aqueous solution by activated carbon prepared from pea shells (*Pisum sativum*),” *Journal of Chemistry*, vol. 2013, Article ID 614083, 9 pages, 2013.
- [55] T. W. Weber and R. K. Chakravorti, “Pore and solid diffusion models for fixed-bed adsorbers,” *AIChE Journal*, vol. 20, no. 2, pp. 228–238, 1974.
- [56] S. Sulaiman, R. S. Azis, I. Ismail et al., “Adsorptive removal of copper (II) ions from aqueous solution using a magnetite nano-adsorbent from mill scale waste: synthesis, characterization, adsorption and kinetic modelling studies,” *Nanoscale Research Letters*, vol. 16, no. 1, pp. 168–217, 2021.
- [57] M. Salman, R. Rehman, U. Farooq, A. Tahir, and L. Mitu, “Biosorptive removal of cadmium (II) and copper (II) using microwave-assisted thiourea-modified *Sorghum bicolor* agrowaste,” *Journal of Chemistry*, vol. 2020, Article ID 8269643, 11 pages, 2020.
- [58] G. Henini, Y. Laidani, S. Hanini, A. Fekaouni, and K. Djellouli Della, “Equilibrium, thermodynamic and kinetic modeling for the adsorption of textile dye (Bemacid blue) onto activated carbon synthesized from olive cores,” *Scientific Study & Research. Chemistry & Chemical Engineering, Biotechnology, Food Industry*, vol. 22, no. 3, pp. 271–288, 2021.
- [59] Y.-S. Ho and G. McKay, “Pseudo-second order model for sorption processes,” *Process Biochemistry*, vol. 34, no. 5, pp. 451–465, 1999.
- [60] A. A. Oyekanmi, A. Ahmad, K. Hossain, and M. Rafatullah, “Adsorption of rhodamine B dye from aqueous solution onto acid treated banana peel: response surface methodology, kinetics and isotherm studies,” *PLoS One*, vol. 14, no. 5, Article ID e0216878, 2019.
- [61] Y. S. Ho, J. C. Ng, and G. McKay, “Kinetics of pollutant sorption by biosorbents,” *Separation and Purification Methods*, vol. 29, no. 2, pp. 189–232, 2000.
- [62] A. Ermolenko, A. Shevelev, M. Vikulova et al., “Wastewater treatment from lead and strontium by potassium polytitanates: kinetic analysis and adsorption mechanism,” *Processes*, vol. 8, no. 2, p. 217, 2020.
- [63] H. P. AkankshaKalra, “Adsorption of dyes from water on to bamboo-based activated carbon-error analysis method for accurate isotherm parameter determination,” *Journal of Water Science and Engineering*, vol. 1, no. 1, pp. 1–11, 2019.
- [64] N. K. Mondal and S. Kar, “Potentiality of banana peel for removal of Congo red dye from aqueous solution: isotherm, kinetics and thermodynamics studies,” *Applied Water Science*, vol. 8, no. 6, pp. 157–212, 2018.
- [65] L. R. Martins, L. Catone Soares, L. V. Alves Gurgel, and L. F. Gil, “Use of a new zwitterionic cellulose derivative for removal of crystal violet and orange II from aqueous solutions,” *Journal of Hazardous Materials*, vol. 424, Article ID 127401, 2022.
- [66] A. C. Sadiq, A. Olasupo, W. S. W. Ngah, N. Y. Rahim, and F. B. M. Suah, “A decade development in the application of chitosan-based materials for dye adsorption: a short review,” *International Journal of Biological Macromolecules*, vol. 191, pp. 1151–1163, 2021.
- [67] Y. Liu, C. Jin, Z. Yang, G. Wu, G. Liu, and Z. Kong, “Recent advances in lignin-based porous materials for pollutants

- removal from wastewater,” *International Journal of Biological Macromolecules*, vol. 187, pp. 880–891, 2021.
- [68] A. G. Pereira, F. H. Rodrigues, A. T. Paulino, A. F. Martins, and A. R. Fajardo, “Recent advances on composite hydrogels designed for the remediation of dye-contaminated water and wastewater: a review,” *Journal of Cleaner Production*, vol. 284, Article ID 124703, 2021.
- [69] H. Ren, Z. F. Cao, Y. Y. Chen, X. Y. Jiang, and J. G. Yu, “Graphene oxide-Bicine composite as a novel adsorbent for removal of various contaminants from aqueous solutions,” *Journal of Environmental Chemical Engineering*, vol. 9, no. 6, Article ID 106769, 2021.
- [70] B. Lapo, J. J. Bou, J. Hoyo et al., “A potential lignocellulosic biomass based on banana waste for critical rare earths recovery from aqueous solutions,” *Environmental Pollution*, vol. 264, Article ID 114409, 2020.
- [71] A. Abdolali, W. Guo, H. Ngo, S. Chen, N. Nguyen, and K. Tung, “Typical lignocellulosic wastes and by-products for biosorption process in water and wastewater treatment: a critical review,” *Bioresource Technology*, vol. 160, pp. 57–66, 2014.
- [72] S. M. Badr and S. Isra’a, “Using agricultural waste as bio-sorbent for hazardous brilliant green dye removal from aqueous solutions,” *Journal of Engineering Science & Technology*, vol. 16, no. 4, pp. 3435–3454, 2021.